

Document downloaded from:

<http://hdl.handle.net/10251/63388>

This paper must be cited as:

Pereira, J.C.; Zambrano, J.; Licausi, M.; Tobar, M.; Amigó Borrás, V. (2015). Tribology and high temperature friction wear behavior of MCrAlY laser cladding coatings on stainless steel. *Wear*. 330:280-287. doi:10.1016/j.wear.2015.01.048.



The final publication is available at

<http://dx.doi.org/10.1016/j.wear.2015.01.048>

Copyright Elsevier

Additional Information

# Tribology and high temperature friction wear behavior of MCrAlY laser cladding coatings on stainless steel

Juan Pereira <sup>a,b,c</sup>, Jenny Zambrano <sup>c</sup>, Marie Licausi <sup>a</sup>, María Tobar <sup>d</sup>, Vicente Amigó <sup>a</sup>

<sup>a</sup> *Instituto de Tecnología de Materiales ITM, Universidad Politécnica de Valencia, España*

<sup>b</sup> *Centro de Investigaciones en Mecánica (CIMEC), Universidad de Carabobo, Venezuela*

<sup>c</sup> *Centro de Investigaciones en Materiales (CIM), Universidad de Carabobo, Venezuela*

<sup>d</sup> *Departamento de Ingeniería Industrial II, Universidade da Coruña, Campus Ferrol, España*

## a b s t r a c t

Temperature can have a significant effect on the extent of wear damage of metallic components. Thermal barrier coatings can improve the high temperature tribological and friction wear behavior. In this work the dry friction and wear behavior at low and high temperature of NiCoCrAlY and CoNiCrAlY laser cladding coatings were evaluated, as well as for the austenitic stainless steel AISI 304 used as substrate. Dense coatings, with good bonding to the substrate was obtained by coaxial laser cladding tracks (40% overlapping), with previously optimized laser parameters. Tribological wear tests were performed by sliding wear at room temperature and 500 °C, with an Al<sub>2</sub>O<sub>3</sub> ball on disk configuration tribometer. The wear scar surface was evaluated by scanning electron microscopy (SEM) and energy dispersive spectroscopy (EDS) microanalysis. The 3D topography of the wear track was determined by inductive contact profilometer which enabled the wear rate calculation. The microstructure of the coatings consists of  $\gamma$ Ni/ $\beta$ -NiAl or  $\gamma$ Co/ $\beta$ -(Co,Ni)Al phases depending on the chemical composition of the alloy, as confirmed by X-ray diffraction (XRD) analysis. The wear test results show a reduction in wear rate at high temperature for all materials tested. For the NiCoCrAlY coating, the high temperature also reduces the friction coefficient, while it significantly increases the friction coefficient of CoNiCrAlY coating. The main damage mode is abrasion and adhesion, caused by the oxide and partially-oxidized particles in the contact surface. The coatings and substrate results were compared, resulting in an improved wear behavior.

*Keywords:* riction Wear MCrAlY Laser cladding Coating

## 1. Introduction

Aircraft and power-generation turbine components are protected by barrier layers of MCrAlY alloys (where M = Ni, Co, Fe or combinations of these). NiCoCrAlY nickel-based and CoNiCrAlY cobalt-based superalloys are widely used as coatings or bond coats between a substrate and a ceramic top in TBCs [1], and are increasingly used for the mechanical components of modern gas turbine engines due to their good adhesion, high modulus, high strength and resistance to high temperature oxidation [2]. NiCoCrAlY and CoNiCrAlY alloys consist of large amounts of Cr with small additions of Y, provided that the solid solution hardens. These effects are quite stable and act as an obstacle on advancing dislocations at the grain boundaries, which cause the typical creep resistance of these alloys [3]. An Al content between 8–15 wt% allows the slow growth of a thermally stable, adherent and continuous oxide layer ( $\alpha$ -Al<sub>2</sub>O<sub>3</sub>) at high temperatures [4,5], and the adherence of the oxide layer to the substrate is influenced by the Y distribution in the alloy before the deposition process [4]. These features can influence the tribological behavior of the coating in applications at low and high temperature.

The laser cladding process can be used to produce dense coatings free of pores and cracks, which improves their high-temperature behavior. The technique can be applied to both small parts and components with complex geometries [6,7]. Process parameters and shielding gas can be controlled to obtain the minimum chemical dilution of the coating alloy with the substrate and to reduce defects [8,9]. Laser cladding can be an alternative to thermal spray process, improving the integrity of the bond coat bond in thermal barrier coatings systems with MCrAlY alloys.

At high temperatures, most metals will inevitably oxidize over a wide range of conditions, and various interactions between materials, the substrate and the atmosphere can be expected, including diffusion,

interdiffusion, decomposition, volatilization and oxide scale growth [10]. The MCrAlY alloys can form stable oxides like  $\alpha$ -Al<sub>2</sub>O<sub>3</sub> and other oxides such as Cr<sub>2</sub>O<sub>3</sub>, NiO, CoO or (Ni,Co)(Cr,Al)<sub>2</sub>O<sub>4</sub> spinel which may improve the performance of the alloy by acting as a thermal barrier.

Wear rate and friction coefficient are important parameters in the performance of the coated components subjected to contact with others at high temperature. The oxidation of metals may influence wear and damage mechanisms [11]. The wear behavior of MCrAlY alloys has been studied by several authors, seeking to improve the high-temperature performance with the inclusion of ceramic particles [12–17]. This study evaluated the friction and wear behavior at high

temperature (500 °C) and room temperature, in static air, of two laser coatings made with NiCoCrAlY and CoNiCrAlY superalloys and optimized laser cladding parameters as a novel alternative to thermal spray coating process. The evaluation of the wear scar surfaces was made by SEM and EDS microanalysis. The profile of wear scars was measured and the wear rate was calculated for both coatings and the substrate.

## 2. Experimental procedure

### 2.1 Materials and laser processing techniques

Gas atomized prealloyed MCrAlY powders supplied by Sulzer Metco (Amdry 365-2 and 995C) were used. NiCoCrAlY alloy was composed mainly of Ni with 23% Co, 17% Cr, 12% Al and 0.42% Y. CoNiCrAlY alloy was composed of Co with 32% Ni, 21% Cr, 8% Al and 0.45% Y. The substrate was a cold rolled stainless steel AISI 304 of 10 mm in thickness. Extensive coatings (30 ~ 30 mm<sup>2</sup>) were obtained using a Nd:YAG solid state laser (Rofin-Sinar DY 022, Germany) in continuous mode with a maximum power of 2.2 kW and a wavelength of 1064 nm; a power ( $P$ ) of 2.2 kW was used in this study. The diameter of the beam focus ( $D$ ) on the part was 4 mm. The XYZ movement was achieved by a robot with 6 degrees of freedom (ABB IRB 2400 unit), velocity ( $V$ ) of 15 mm/s and overlapping ratio in laser scan of 40%. Powder was supplied per unit length of 25 mg/mm and provided with a coaxial annular nozzle (Precitec YC50) and a Sulzer Metco Twin 10-C powder feeder. Helium (20 l/min) was used as a shielding and powder carrier gas.

### 2.2 Powder characterization, coating microstructure and hardness

For powder characterization, a laser beam was diffracted through particles suspended in distilled water using a Mastersizer 2000 laser diffractometer to obtain the variations in particle size. The powder morphology and chemical composition was obtained by scanning electron microscopy (SEM) and energy dispersive spectroscopy (EDS). The measurements of X-ray diffraction were carried out on a Philips X'pert using monochromatic Cu K $\alpha$  radiation ( $\lambda$  0.15406 nm). The patterns of X-ray diffraction were in the range of  $2\theta$  from 20 to 90 and were analyzed using X'Pert Plus software (PANalytical). Microstructural characterization of the coating was carried out on a cross section, which was previously cut and metallographically prepared for analysis, using backscattered electron images (BSE) of the microstructure at different magnifications in a Jeol JSM6300 scanning electron microscope. Microanalysis to quantify the chemical composition was performed by EDS using an X-Max Oxford Instruments microanalysis system with an X-ray detector of 20  $\mu$ m<sup>2</sup>. A microhardness tester Shimadzu HMV-2 (automatic measurement) was used to measure the hardness in the coating and substrate. Three indentations were made for the average value of each point, the measurements were performed with a load of 980.7 mN and an application time of 10s (HV0.1 scale), the spacing between indentations was 100  $\mu$ m and the first measurement was made at 50  $\mu$ m from the surface coating.

### 2.3 Friction and wear test

The wear tests were performed with a high-temperature tribometer with a ball on disc configuration, manufactured by MICROTTEST MT2/60/SCM/T (Spain), according to ASTM G99-03 and DIN 50324 standards. Four wear tests were made for each material/ condition. Before the tests, the coating surface was ground to a finish of 500 grit SiC paper ( $R_a = 0.17 \pm 0.05 \mu$ m), and were cut into samples of 15 ~ 15 mm. Al<sub>2</sub>O<sub>3</sub> grade 25 balls (5 mm diameter, 0.05

$\mu\text{m}$  and hardness of 2400 HV) manufactured by Precision Ball & Gauge Co. (England) were used as counterpart material, due to the stability of this material at high temperature. The test parameters were: contact load of 10 N, speed 0.1 m/s, sliding distance of 500 m, temperatures of 24 1C (RT) and 500 1C (HT) in static air (65% RH), the heat rate for RaHT wear tests was 20 1C/min. A radius of wear track of 5 mm was used for all tests.

The temperature near the ball-sample contact area was measured with a contact type 'K' thermocouple with grounded hot junction of Inconel alloy, and recorded during the test. Wear profiles were measured with an inductive contact profilometer (range 2.5 mm) Taylor Hobson Talysurf 50 to obtain the 3D topography of the wear track. The average wear area was determined through the measurement of four different profiles of the wear track. The measurements were done on four wear tested samples. The wear rate ( $W_r$ ) was calculated using the following formula:

$$W_r = \frac{P \times A}{F \times L} \quad (1)$$

where  $W_r$  is the rate of wear in  $\text{mm}^3/(\text{N m})$ ;  $P$  is the mean scar circumference in mm;  $A$  is the average wear area in  $\text{mm}^2$ ;  $F$  is the applied normal load in N; and  $L$  is the sliding distance in m.

### 3. Results and discussion

#### 3.1 Powder characterization

Two prealloyed MCrAlY alloys powders were used in this study. Both powders have a spherical morphology (Fig. 1a and b) typical of the gas atomization process, and particle size analysis of the powder revealed a mean particle size of 55.3  $\mu\text{m}$  for NiCoCrAlY powder and 64.7  $\mu\text{m}$  for CoNiCrAlY powder. The Gaussian particle size distribution can be seen in Figs. 1c and d. The morphology and size of the powder is very important for the coaxial laser cladding processing because the flowability of the powder influences the quality of the coating. Two phases can be distinguished in each powder's feedstock according to XRD analysis, consisting of  $\gamma$ -Ni (Cr)/Co(Ni,Cr) and  $\beta$ -NiAl/(Co,Ni)Al depending on the base element of the alloy.

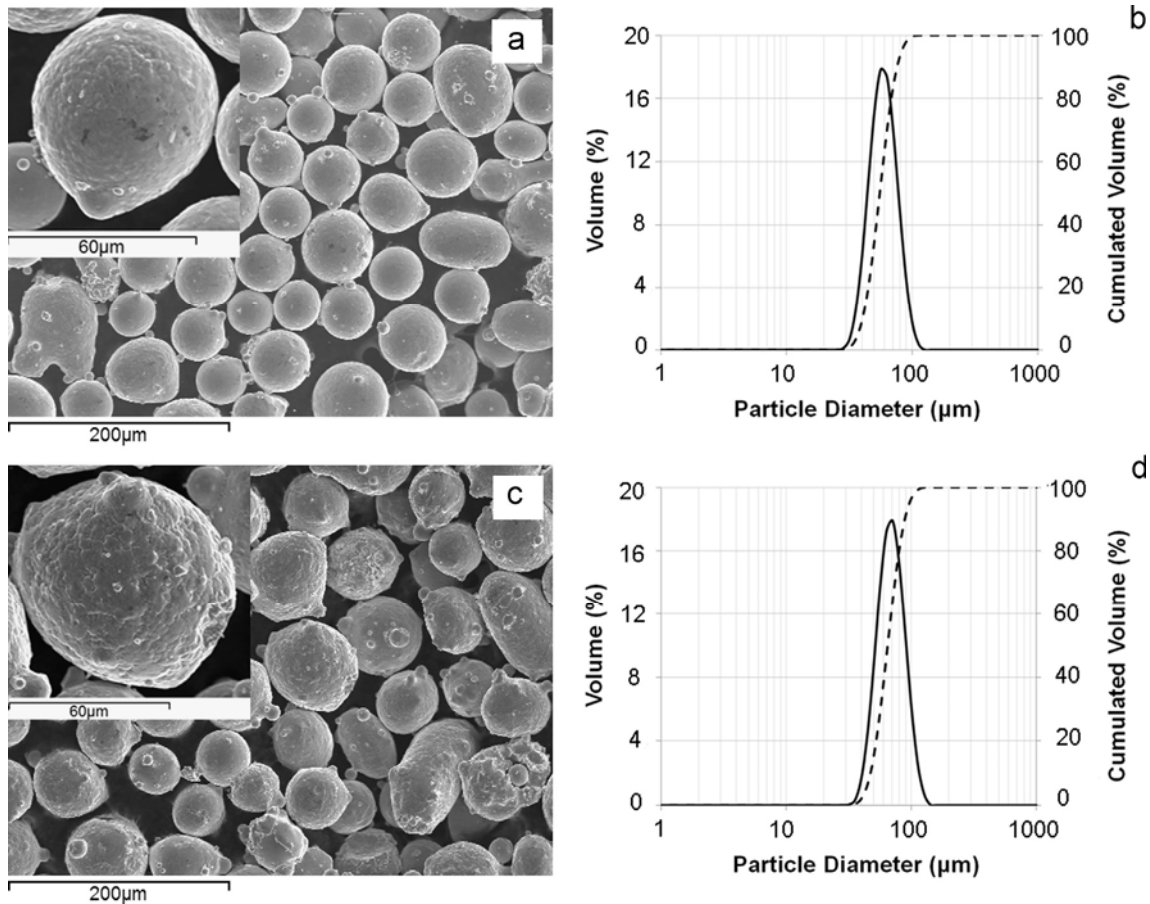


Fig. 1. Powder feedstock characterization. Morphology detail in SEM (20 kV SEM) of a) NiCoCrAlY powder c) CoNiCrAlY powder. And particle size distribution of b) NiCoCrAlY powder d) CoNiCrAlY powder.

### 3.2 Geometry, microstructure and hardness of the coatings

Many variables are involved in the laser cladding process, which requires studying the geometry and chemical dilution of single clad tracks before creating extensive overlapping coatings. In previous work [18–20], laser cladding parameters were studied on a NiCoCrAlYTa alloy to obtain an adequate aspect ratio, homogeneity, low dilution and a good metallurgical bond with the substrate. In this study, high velocity, high powder feed rate and high laser power were combined to build overlapping coatings. The specific laser energy ( $36.67 \text{ J/mm}^2$ ) was combined with a laser with a 4-mm diameter allowed us to obtain adequate coatings.

The initial coating thickness for the NiCoCrAlY alloy was  $832 \pm 45 \mu\text{m}$  (Fig. 2a). This provided a dense coating with a homogeneous structure, and minimum dilution with the substrate was observed. The thickness of the CoNiCrAlY alloy coating was  $715732 \mu\text{m}$  (Fig. 2b), with a dendritic columnar structure and small pores.

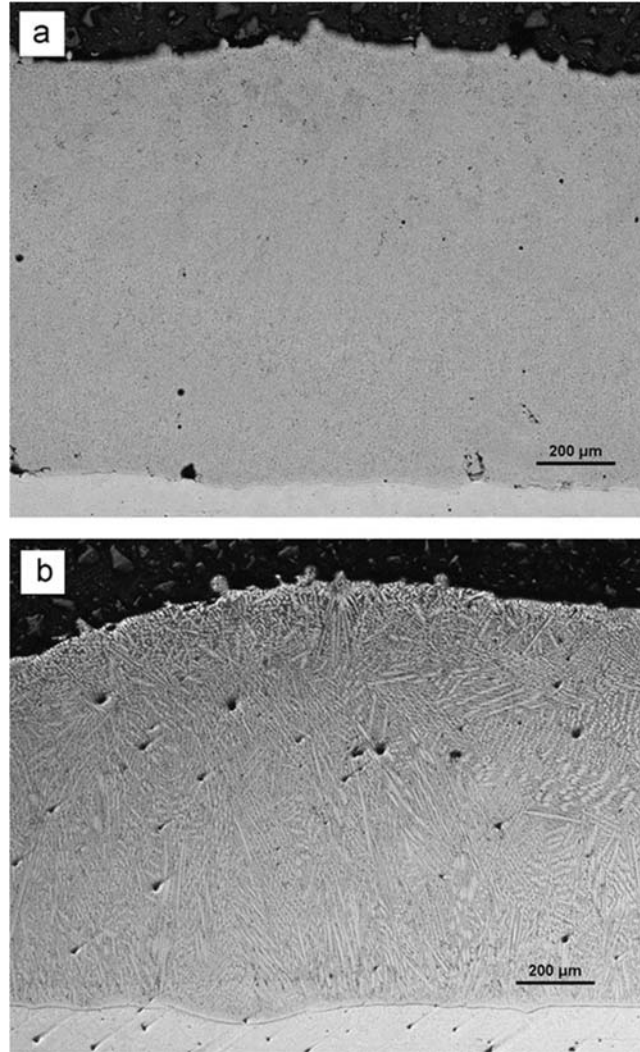


Fig. 2. Optical micrographs of the laser cladding coating/interface a) NiCoCrAlY alloy b) CoNiCrAlY alloy.

The coatings' microstructures are composed of two principal phases, a  $\gamma$  matrix phase and  $\beta$  phase. The NiCoCrAlY coating has a cellular dendritic structure (Fig. 3a), and EDS microanalysis revealed a dendritic  $\gamma$ -Ni matrix phase with Cr and Co elements in solid solution and an interdendritic  $\beta$ -NiAl phase (dark) rich in Al with Co in solid solution. Ni-Y rich zones are present in some  $\gamma/\beta$  grain boundaries. In the CoNiCrAlY coating, a columnar dendritic structure with planar solidification front was observed (Fig. 3b). In this case, the interdendritic phase (dark) is shorter due to the lower content of Al in this alloy. EDS analysis also suggests a hypoeutectic solidification with  $\gamma$ -Co(Ni,Cr) and  $\beta$ -(Co,Ni)Al interdendritic phase. The  $\gamma/\beta$  coatings' microstructures are confirmed by XRD analysis (Fig. 4).

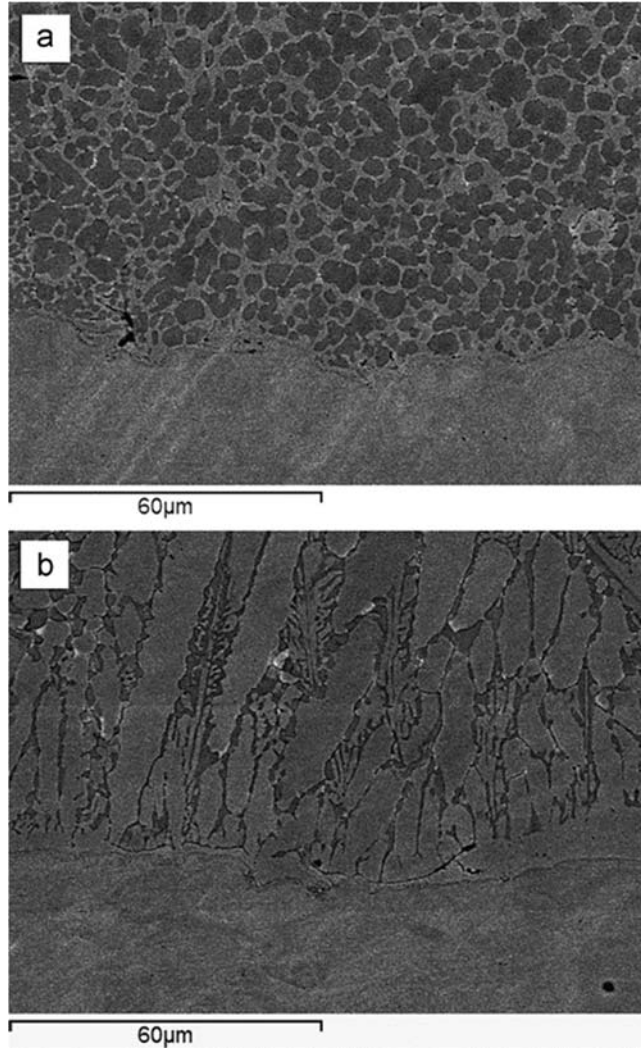


Fig. 3. BSE-SEM micrographs of the interface coating/substrate a) NiCoCrAlY alloy b) CoNiCrAlY alloy.

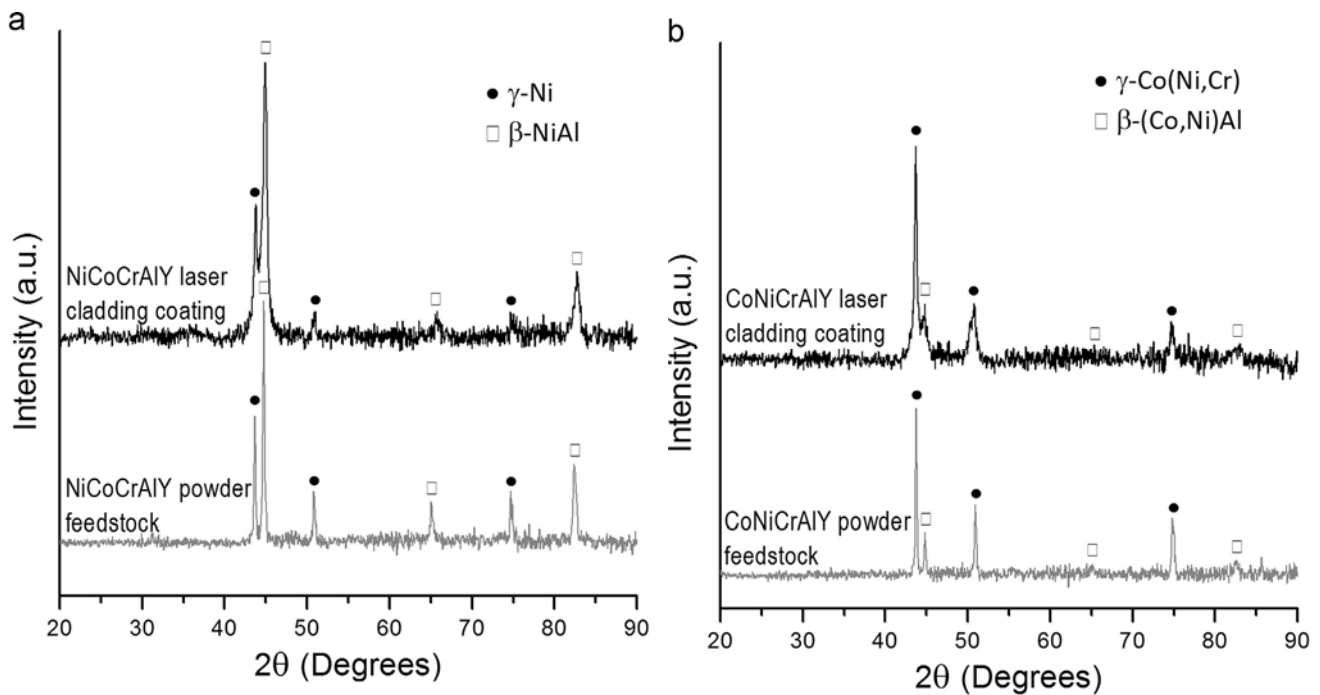


Fig. 4. XRD Analysis a) NiCoCrAlY powder and LC coating b) CoNiCrAlY powder and LC coating.

The evolution of hardness from the coatings' surface to the substrate is shown in Fig. 5, and summarized results in Table 1. The hardness of the coatings is higher than the substrate, and the hardness of the NiCoCrAlY laser cladding coating is higher than the CoNiCrAlY coating one. This hardness behavior difference between the coatings may be due to the coating microstructure and phase composition, founded more beta phase in the coating with higher aluminum content (NiCoCrAlY), and different dendritic structure. The beta phase is harder than the gamma phase matrix [21] in MCrAlY superalloys.

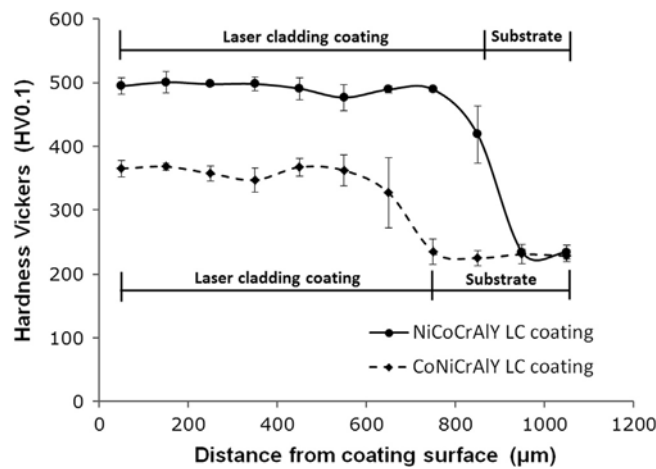


Fig. 5. Coatings/substrate hardness evolution.

Table 1. Average hardness results for coating and substrate.

Coating/su	Vickers	Standard
NiCoCrAlY	492	7.1
CoNiCrAlY	361	7.3
AISI 304	230	3.4

### 3.3 Friction and wear behavior

The friction coefficients and the wear rates were obtained from wear tests. Fig. 6 shows the behavior of the friction coefficient, for both alloys, in function of the sliding distance, obtained at room temperature and high temperature (500 °C) in static air. During testing, a slight instability in the initial friction coefficient can be attributed to the removal or redistribution of the particles on the contact surface. The NiCoCrAlY friction coefficient decreases slightly at high temperatures going from  $0.49 \pm 0.08$  (RT) to  $0.45 \pm 0.01$  (HT), possibly due to the formation of oxides and other intermetallic compounds which reduce the adhesion phenomenon and plowing on the coating. While for the CoNiCrAlY coating the plowing phenomenon and adhesion are increased on the surface coating at high temperature, greatly increasing the friction coefficient going from  $0.46 \pm 0.03$  (RT) to  $1.00 \pm 0.30$  (HT). Both coatings have similar frictional behaviors at room temperature but radically different at high temperature.

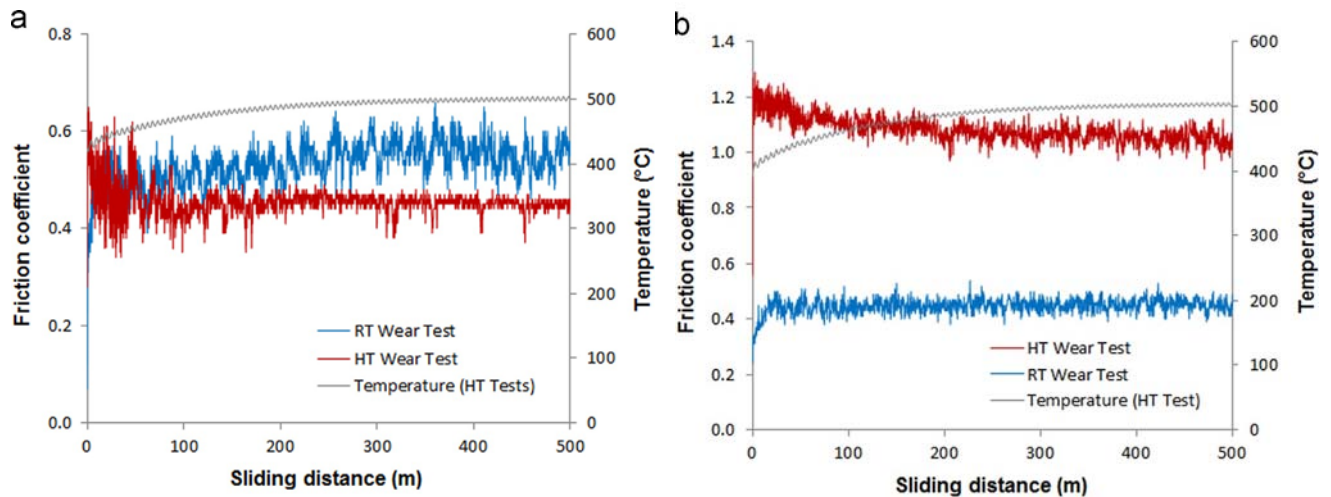


Fig. 6. Friction coefficient behavior a) NiCoCrAlY coating b) Coating CoNiCrAlY.

The cobalt-based super alloy has a higher content of cobalt and chromium with aluminum content lower than the nickel-base alloy, which affects the kinetics of oxidation of the contact surface and the frictional behavior, increasing the resistance to plowing at high temperature. The Fig.7 shows the SEM micrographs of coatings' wear scar, and Fig. 8 shows a detail of

wear surface at high temperature with EDS microanalysis. At room temperature, the main damage mode for the NiCoCrAlY coating (Fig. 7a) is abrasion; at the edges of the track the material is plastically deformed in CoNiCrAlY coating (Fig. 7c), this behavior at room temperatures is common in metallic materials [22]. At high temperature, it appears that the primary mode of damage is abrasion for the NiCoCrAlY coating. Wear debris induced the formation and removal of oxides during the wear process (Fig. 7b and d) with a higher accumulation and adhesion of oxides ( $\text{Al}_2\text{O}_3$ ,  $\text{Cr}_2\text{O}_3$ , NiO) (Fig. 8a and b), possible material delamination can also be seen in certain areas of the track (Fig. 8a). Both coatings suffered plastic deformation due the increased ductility at high temperature.

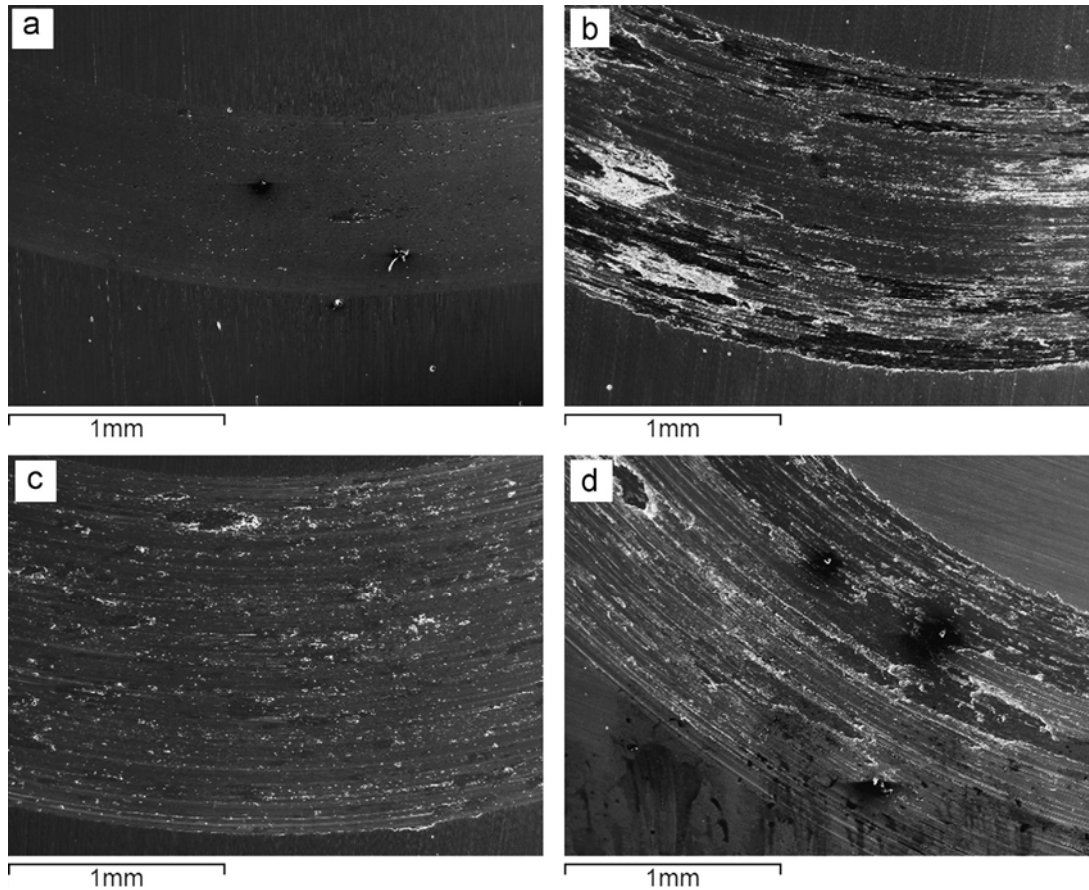


Fig. 7. SEM micrographs (20 kV 50 ~ SE) of wear tracks a) NiCoCrAlY RT test b) NiCoCrAlY HT test coating c) CoNiCrAlY RT test d) CoNiCrAlY HT test.

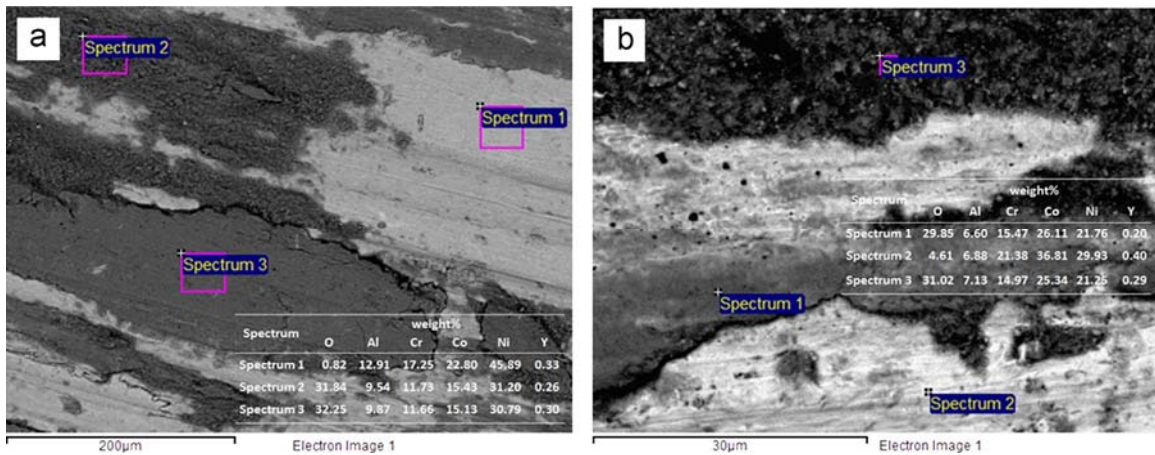


Fig. 8. SEM micrographs (20 kV BSE mode) of wear tracks a) NiCoCrAlY HT test b) CoNiCrAlY HT.

The continuous formation and destruction of the transfer layer influences the fluctuation (amplitude) of the friction coefficient (Fig. 6). Material removed in HT tests is lower due to the formation of oxides and partly oxidized alloy particles at high temperatures which reduce the metal-metal contact and thus reduces the wear rate [12].

3D profiles of the wear track of the coatings are shown in Fig. 9. Differences were observed in the width and roughness of the wear tracks obtained at high temperature. For each sample, the 2D profile of the wear scar was obtained (Fig. 10), and the volume of material removed was calculated from these profiles. The results of the wear test indicate that the RT removed volume is higher than the HT removed volume, so that the wear rate is reduced by 39% for the NiCoCrAlY coating and 60% CoNiCrAlY coating at high temperature. In the substrate the trend is similar; the wear rate is reduced by 84.6% at high temperature. In 2D wear scar profile the plastic deformation at the track edge is observed for CoNiCrAlY coating and AISI 304 substrate samples tested at high temperature (Fig. 10). The counterbody analysis after HT tests reveal that in ball surface small abrasion marks (may be microplowing) and dark color are observed (with flat and undeformed surface), with small residues of coating oxides (3-body-abrasion). Summarized results of the friction coefficient and wear volume are shown in Table 2. At high temperature the laser cladding coatings and substrate have a better frictional wear behavior due to the formation of compacted layers of oxide and partially-oxidized alloy particles on the sliding surface that reduce the wear [11].

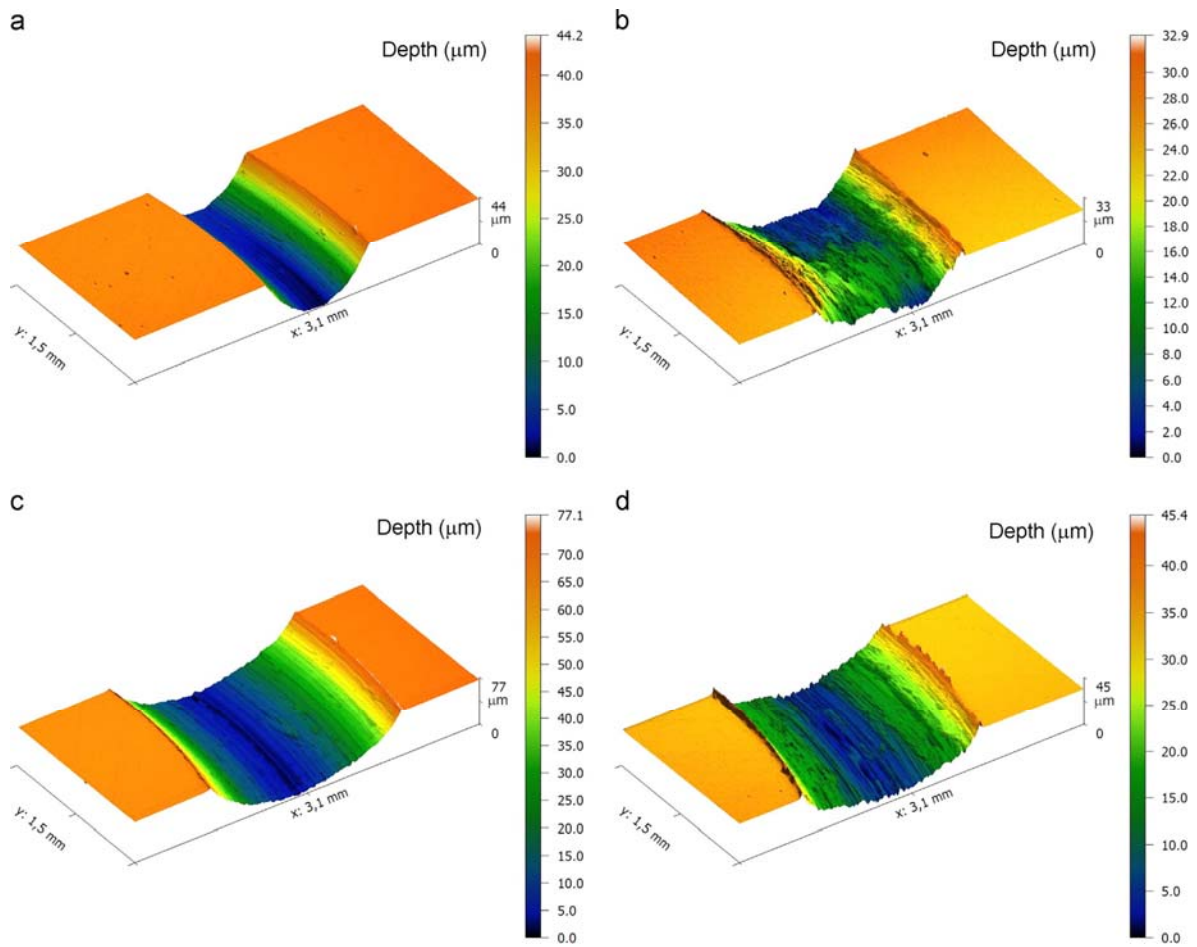


Fig. 9. 3D profile of wear tracks a) NiCoCrAlY RT b) NiCoCrAlY HT c) CoNiCrAlY RT d) CoNiCrAlY HT.

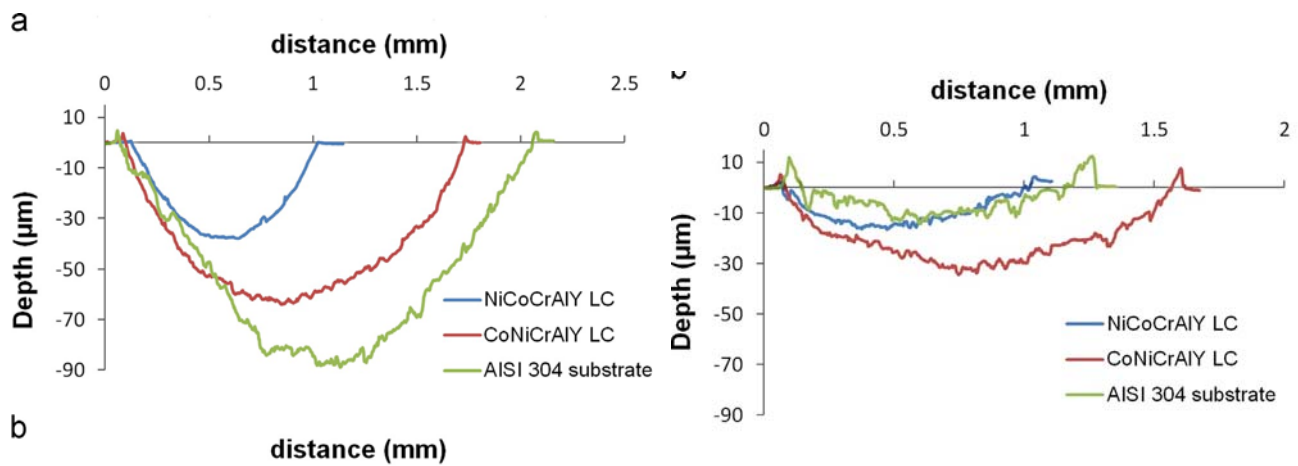


Fig. 10. 2D profile of wear tracks a) RT tests b) HT tests.

Table 2. Wear test results.

Coating/ substrate material	Temperature test (°C)	Friction coefficient	Removed volume (mm <sup>3</sup> )	Wear rate, $W_r$ (10 <sup>-4</sup> mm <sup>3</sup> /(N m))
NiCoCrAlY	24 (RT)	0.49 ± 0.08	0.82 ± 0.09	1.63 ± 0.18
	500 (HT)	0.45 ± 0.01	0.50 ± 0.18	0.99 ± 0.36
CoNiCrAlY	24 (RT)	0.46 ± 0.03	2.36 ± 0.24	4.73 ± 0.47
	500 (HT)	1.00 ± 0.30	0.94 ± 0.23	1.89 ± 0.46
AISI 304	24 (RT)	0.60 ± 0.11	3.45 ± 0.39	6.89 ± 0.78
	500 (HT)	0.49 ± 0.04	0.53 ± 0.11	1.06 ± 0.22

Room temperature wear rate of NiCoCrAlY laser cladding coating is similar to reported by previous work [15,17] and lower than wear rate reported for thermal spray TBCs [23]. At high temperature the nickel-based laser cladding coating has lower wear rate than the substrate, but the cobalt-based coating has a higher wear rate. This is due primarily to a combination of wear mechanisms at high temperature: abrasion, adhesion by the oxide particles (as see in Fig. 8a), may be surface fatigue and plastic deformation due to the high ductility showing both the substrate and the NiCoCrAlY coating at temperature test (500 °C), also the difference in the aluminum content and solid solution matrix phase between coatings alloys can affect the wear behavior and hence a lower wear rate is obtained. It is important to investigate the friction and wear behavior at higher temperatures (600–1100 °C) to determine whether changing the wear mechanisms observed in this investigation.

#### 4. Conclusions

1. The results confirmed that the coaxial laser cladding is a good alternative to the thermal spray coating process and that the MCrAlY coatings can improve the friction and wear behavior of austenitic stainless steels. The friction coefficient decreases in NiCoCrAlY coating at high temperature, while it increases significantly in the CoNiCrAlY coating.
2. The primary mechanism for material removal at high temperature is abrasion due to the contribution of the action of oxidized particles or residues formed at high temperature, although oxide adhesion, surface fatigue and material plastic deformation due the ductility is displayed during the tests. At low temperature the dominant wear mechanism is abrasion with some adhesion and delamination of the coating material. At high temperature the NiCoCrAlY laser cladding coatings obtained have better frictional wear behavior, reducing the wear rate and friction coefficient obtained on the substrate.

#### Acknowledgments

The authors acknowledge the financial support of the Ministry of Science and Innovation of the Government of Spain through research project MAT2011-28492-C03 and the

Generalitat Valenciana through ACOMP/2013/114 support. Professor Juan Carlos Pereira Falcón thanks the University of Carabobo (Grant CD- 3997-2011) for the financial support to pursue his doctoral studies at the UPV. Furthermore, the authors thank Dr. José Luis Jordá for the XRD analysis.

## References

- [1] U. Schulz, A. Leyens, K. Fritscher, Some recent trends in research and technology of advanced TBCs, *Aerosp. Sci. Technol.* 7 (2003) 73–80.
- [2] M. Pomeroy, Coatings for gas turbine materials and long term stability issues, *Mater. Des.* 26 (2005) 223–231.
- [3] F. Tancret, H. Bhadeshia, D. MacKay, Design of a creep resistant nickel base superalloys for power plant applications, part 1 – mechanical properties modelling, *Mater. Sci. Technol.* 19 (2003) 283–290.
- [4] T. Nidjam, C. Kwakernaak, W. Sloof, The effects of alloy microstructure refinement on short-term thermal oxidation of NiCoCrAlY alloys, *Metall. Mater. Trans. A* 37 (3) (2006) 683–693.
- [5] G. Marginean, D. Utu, Cyclic oxidation behavior of different treated CoNiCrAlY coatings, *Appl. Surf. Sci.* 258 (2012) 8307–8311.
- [6] J. De Damborenea, A. Vázquez, Laser cladding of high-temperature coatings, *J. Mater. Sci.* 28 (1993) 4775–4780.
- [7] R. Vilar., Laser cladding, *J. Laser Appl.* 11 (1999) 64–79.
- [8] F. Vollertsen, K. Partes, J. Meijer, “State of the art of laser hardening and cladding”, in: *Proceeding of WLT Conference on Lasers in Manufacturing, 2005*, p. S. 281.
- [9] J. Dutta Majumdar, I. Manna, Laser material processing, *Int. Mater. Rev.* 56 (2011) 341–388.
- [10] D. Young, *High Temperature Oxidation and Corrosion of Metals*, Elsevier, Amsterdam, 2008, pp: 4-8 and 15-21.
- [11] F. Stott, High-temperature sliding wear of metals, *Tribology International.* 35 (2002) 489–495.
- [12] L. Zhao, M. Parco, E. Lugscheider, war behaviour of Al<sub>2</sub>O<sub>3</sub> dispersion strengthened MCrAlY coating, *Surf. Coat. Technol.* 184 (2004) 298–306.
- [13] H. Wang, D. Zuo, M. Wang, G. Sun, H. Miao, Y. Sun, High temperature frictional wear behaviors of nano-particle reinforced NiCoCrAlY cladded coatings, *Trans. Nonferrous Met. Soc. China* 21 (2011) 1322–1328.
- [14] H. Wang, D. Zuo, X. Li, M. Wang, Y. Zhao, Effects of nano-Al<sub>2</sub>O<sub>3</sub>p on high temperature frictional wear behaviors of NiCoCrAlY cladded coatings, *Adv. Mater. Res.* 426 (2012) 40–43.
- [15] G. Chun, C. Jianmin, Y. Rungang, Z. Jiansong, Microstructure and high temperature wear resistance of laser cladding NiCoCrAlY/ZrB<sub>2</sub>, *Rare Met. Mater. Eng.* 42 (8) (2013) 1547–1551.
- [16] Z. Hu, J. Liu, C. Guo, J. Zhou, S. Zhang, Microstructure and wear resistance of laser cladding NiCoCrAlY/HfB<sub>2</sub> coating at elevated temperature, *China Surf. Eng.* 2

- (2012) 69–74.
- [17] D. Wang, Z. Tian, S. Wang, L. Shen, Microstructure and wear resistance of laser cladding nano-Al<sub>2</sub>O<sub>3</sub>/MCrAlY composite graded coating on TiAl alloy, *Appl. Mech. Mater.* 217 (2012) 1350–1353.
  - [18] J. Pereira, J. Candel, J. Amado, V. Amigó, Geometric and microstructural analysis of laser clad NiCoCrAlYTa coating on stainless Steel AISI 316L, *Rev. LatinAm. Metal. Mater.* 34 (2014) 209–217.
  - [19] J. Pereira, J. Candel, J. Amado, V. Amigó, Caracterización microestructural de recubrimientos NiCoCrAlYTa obtenidos por láser coaxial y por refusión láser sobre AISI 316L, *Rev. Colomb. Mater.* 5 (2014) 127–132.
  - [20] M. Tobar, J. Amado, A. Yáñez, J. Pereira, V. Amigó, Laser cladding of MCrAlY coatings on stainless steel, *Phys. Procedia* 56 (2014) 276–283.
  - [21] D. Kim, S. Cho, J. Choi, J. Koo, C. Seok, M. Kim, Evaluation of the degradation of plasma sprayed thermal barrier coatings using nano-indentation, *J. Nanosci. Nanotechnol.* 9 (2009) 7271–7277.
  - [22] K. Holmberg, H. Ronkainen, A. Laukkanen, K. Wallin, Friction and wear of coated surfaces-scales, modelling and simulation of tribomechanisms, *Surf. Coat. Technol.* 202 (2007) 1034–1049.
  - [23] G. Bolelli, V. Cannillo, L. Lusvardi, T. Manfredini, Wear behaviour of thermally sprayed ceramic oxide coatings, *Wear* 261 (2006) 1298–1315.